Aerosol and Air Quality Research

ORIGINAL RESEARCH
https://doi.org/10.4209/aaqr.230123

Experimental and Computational Analysis of Surgical Mask Effectiveness Against COVID-19 in Indoor Environment

Chin Yan Suen[1†], Helen Hoi Ling Kwok[2†], Yuk Hang Tsui[3,4†], Ka Hei Lui[5,6], Hong Hang Leung[1], Ka Wo Lam[1], Karen Pik Shuen Hung[1], Joseph Kai Cho Kwan[1*], Kin Fai Ho[6*]

[1] Division of Environment and Sustainability, The Hong Kong University of Science and Technology, Hong Kong
[2] Institute for the Environment, Hong Kong University of Science and Technology, Hong Kong University of Science and Technology, Hong Kong
[3] Department of Mathematics, The Hong Kong University of Science and Technology, Hong Kong
[4] Department of Computer Science and Engineering, The Hong Kong University of Science and Technology, Hong Kong
[5] Department of Chemical and Biological Engineering, The Hong Kong University of Science and Technology, Hong Kong
[6] The Jockey Club School of Public Health and Primary Care, The Chinese University of Hong Kong, Hong Kong

ABSTRACT

An experiment coupled with a computational analysis was conducted to investigate the effectiveness of surgical masks, which include KF94 and ASTM Level 1, in an indoor environment. The KF94 mask sample shows the highest filtration efficiency (99.9%) in the analysis. The simulation is consistent with the experimental results as the concentration of sodium chloride (NaCl) droplets is $< 4\%$ on average in the room. The ultraviolet-C (UVC) irradiation and dry heating samples are shown to retain the highest filtration efficiencies ($> 97\%$) after 3 disinfection treatment cycles. All methods (boiling, steaming, ethanol treatment, and dry heating) effectively reduce the *S. aureus* load by 99.99%. The UVC irradiation shows exposure to 450 $\mu W\ cm^{-2}$ for 10 minutes can effectively eliminate all *S. aureus* on the mask materials. Simulation shows the reduction in overall NaCl and carbon dioxide (CO_2) levels is directly proportional to the filtration efficiency and the effectiveness of reused masks is also directly proportional to the filtration efficiency. The proxy indicator (CO_2) for aerosol particles demonstrates that very fine respiratory droplets can penetrate the mask after reaching a steady state. The CO_2 concentration increase shows that aerosol particles are accumulated under adequate ventilation and further pose the risk of infection. The NaCl droplets (2%) simulation shows that respiratory droplets have infiltrated the mask, but the mask demonstrates a higher ability to block the NaCl droplets and prevent their penetration. The findings suggest a need to revise the existing regulation of the control policy.

Keywords: Surgical mask, Disinfection methods, COVID-19, Computational fluid dynamics, Indoor air quality

1 INTRODUCTION

The COVID-19 pandemic is caused by the severe acute respiratory syndrome coronavirus 2 (SARS-CoV-2), the virus responsible for the coronavirus disease of 2019. This virus is detrimental to mankind, threatens to overload the public healthcare system, and further jeopardizes the

OPEN ACCESS

1Received: June 19, 2023
Revised: July 28, 2023
Accepted: August 14, 2023

*** Corresponding Authors:**
Joseph Kai Cho Kwan
joekwan@ust.hk
Kin Fai Ho
kfho@cuhk.edu.hk

† These authors contributed equally to this work

Publisher:
Taiwan Association for Aerosol Research
ISSN: 1680-8584 print
ISSN: 2071-1409 online

global economy. The World Health Organization (WHO) approved that wearing surgical masks is effective in controlling the spread of respiratory virus diseases in society (WHO, 2020).

During the pandemic, the high demand for personal protective equipment (PPE) drives the need to explore the possibility to reuse and extend the lifespan of single-use disposable PPE equipment, especially for items such as N95 respirators and surgical masks. The supplies of surgical masks usually lag behind because of the large demand on a global scale (Ishack and Lipner, 2020). In order to provide sufficient protection to our citizens, the possibility of reusing surgical masks using different disinfection methods is a prime target in short term. The disinfection techniques include dry heating (100°C), steaming, boiling, autoclave, soaking in ethanol (75 and 95% concentration) or household detergent, and irradiation under ultraviolet (UVC) light. A previous study showed that the aforementioned disinfection treatments were effective, except when household detergent was used (Block, 2001). Nevertheless, the current understanding of disinfection efficiency, as well as the structural and property changes of surgical masks after various disinfection treatments, is limited.

There are several universally recognized standards (ASTM-F, EN14683, KF, and YY0469) for testing the quality of surgical masks (WHO, 2020). The methods involve testing the filtration efficiency, breathability and liquid repellency in general. Filtration efficiency measures the effectiveness of filtering particles from 0.1 to 3.0 μm aerodynamic size. The cut-off sizes in the aforementioned tests are classified as particulate filtration efficiency (PFE) and bacteria filtration efficiency (BFE) (Rengasamy *et al.*, 2017). Latex sphere is used in the PFE filtration test under the ASTM standard (ASTM International, 2017), whereas the KF, YY0469 and the other standard (e.g., NIOSH) all use sodium chloride aerosols throughout the tests (NIOSH, 2007; CFDA, 2011; Jung *et al.*, 2014). The phenomenon is that droplets start to evaporate as soon as exposed to the air and terminal velocity decreases with smaller droplet size (Xie *et al.*, 2007). This implies that small-size droplets can travel longer distances and potentially lead to a higher risk of infection if the droplet nuclei are a pathogen. The main indicators to assess the level of destruction under different disinfection treatments are filtration efficiency and liquid repellency in this study. Structural changes for the filtration layer were also observed and verified after treatments to understand the disinfection effectiveness of surgical masks in the tests.

The World Health Organization (WHO) and the United States Centers for Disease Control (CDC) recommend using facial coverings and social distancing to curb the virus spreading. However, more research is needed to update the guidelines from time to time. Computational fluid dynamics (CFD) simulation is a representative approach for air distribution analysis that can be used to investigate indoor air quality (IAQ) under different configurations without conducting multiple costly full-scale field measurements (Nielsen, 2015). The exhaust airflow variations in the kitchens on different floors were analyzed using CFD (Yang *et al.*, 2021). The CFD simulations were conducted to assess IAQ and thermal comfort of multiple office floors for design analysis of fresh air shafts (Kwok *et al.*, 2022). Extensive research has been conducted on ventilation performance and IAQ using CFD simulations (Chen, 2009).

Different studies have attempted to quantify the impact of facial masks in limiting the transmission of pathogen-bearing droplets. Schade *et al.* (2021) studied the dispersion of small aerosols and carbon dioxide (CO_2) in a concert hall to estimate the risk of virus infection. The results indicated a correlation between the CO_2 concentration and the spatial dissipation of aerosols. CO_2 monitoring in a concert hall or theater's audience can support COVID-19 infection risk estimation. Moreover, CO_2 was used as a proxy to estimate SARS-CoV-2 exposure on the terrace of a restaurant (Rivas *et al.*, 2022). A previous study using CFD analysis showed airflow and temperature distribution patterns could determine the dispersal of droplet particles inside a grocery store. The results demonstrated that the distance traveled by particles is affected by mechanical ventilation significantly (Zhang *et al.*, 2022a). A study used high-fidelity CFD simulations to investigate particulate transport in human saliva, and the effectiveness of a medical mask and a non-medical mask were compared based on their geometry (Khosronejad *et al.*, 2020). Each of the five simulations conducted requires 1000 CPUs for about 4 months of CPU time on average. A past study investigated the impact of ambient wind and relative humidity on the SARS-CoV-2-laden droplets using CFD simulation (Feng *et al.*, 2020). The findings suggested that environmental wind conditions have significant impacts on droplet transport and deposition. Masks are effective to

reduce the suspension of small droplets in the air. Using 32 CPU cores, it took approximately 8 hours to complete one simulation. Although CFD simulation has been extensively used to study thermal comfort and indoor air quality (Chen *et al.*, 2015), there are currently limited studies on using CFD simulation coupled with mask disinfection treatment to explore the impact of mask effectiveness in indoor environments. The developed approaches by previous research require high computational costs to conduct simulations. It is expensive to conduct simulations on multiple masks and consider different scenarios. A methodology to estimate the mask effectiveness of different types of new and reused masks at a lower computational cost is required.

The aims of this study are to: 1) investigate surgical mask performance under pre-conditioned and indoor environments with occupants; 2) evaluate the reusability of masks based on conventional experimental procedures; 3) and simulate the relationships between the effectiveness of masks and indoor air quality using computational fluid dynamics simulation. Section 2 illustrates the proposed methodology to quantify mask effectiveness of new and reused masks using experimental and computational approaches. Section 3 presents the experimental and simulated results of the sample masks. The impacts of mechanical ventilation and mode of transmission on mask effectiveness are discussed in this section. Section 4 includes the conclusion, limitations of the study and possible future studies.

2 METHODS

An experimental and simulation-based methodology is proposed to quantify surgical mask effectiveness in an indoor environment and its reusability, as illustrated in Fig. 1. Performance and reusability of the masks are evaluated by filtration efficiency test, bactericidal test, hydrophobicity test and structural deformation investigation. Based on experimental results, CFD simulations were conducted to quantify mask effectiveness in an indoor environment.

2.1 Experimental Setup

2.1.1 Mask samples

ASTM (level 1) surgical masks are commonly used and recommended by World Health Organization (WHO) for protective covering for the face (WHO, 2023). The KF94 is one of the common masks used in Hong Kong (Zhang *et al.*, 2022b). Two ASTM (level 1) surgical masks and one KF94 were selected as the test subjects for mask effectiveness analysis. The fiber materials of these samples were sectioned (5 × 5 cm) for physical characteristic measurement. ASTM (level 1, A. R. Medicom Inc. [Asia] Ltd.) surgical mask was chosen as the test subject for reusability study

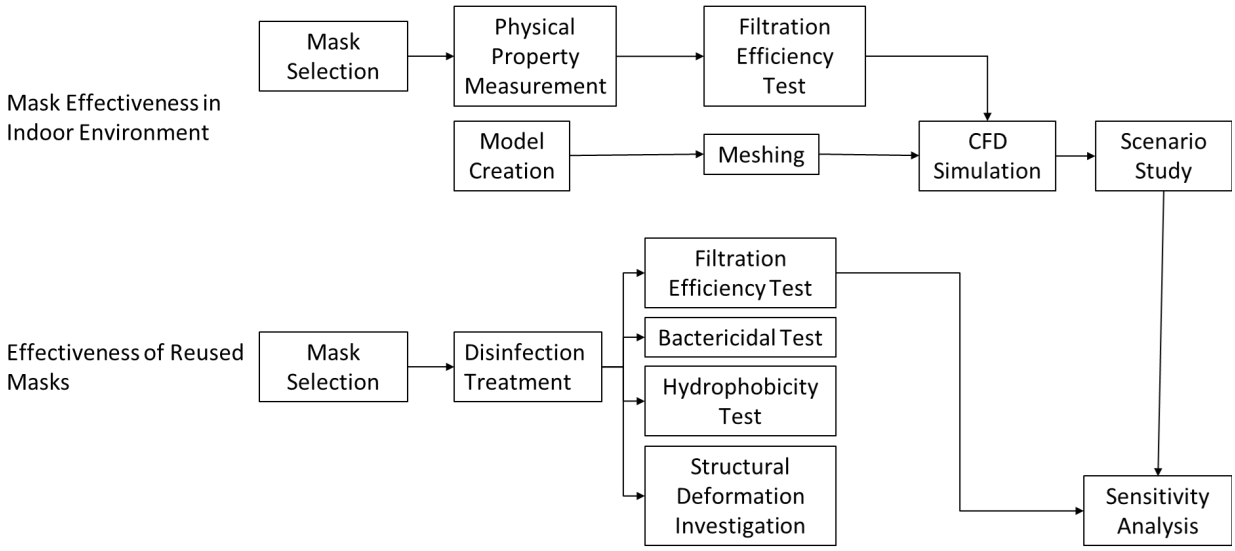

Fig. 1. Experimental and simulation-based methodology for mask effectiveness analysis.

due to its popular use (e.g., hospitals) worldwide. The test samples were labeled and randomly assigned to various treatment groups. Each treatment group (n = 3 for each type of mask) was sterilized by one of the methods as described in Table S1.

2.1.2 Filtration efficiency test

The test illustrated in Fig. S1 was used to determine the material performance based on the filtration efficiency of non-viable particles. Sodium chloride particles were used to mimic sub-micron exhaled droplets generated from coughing and talking. The 2% sodium chloride solution (NaCl) was aerosolized by a Particle Generator (TSI Model 8026) with a count median diameter of 0.04 μm (nominal) and a geometric standard deviation of 2.2 μm (nominal). This instrument can produce particles in the range of a few tens of nanometers to approximately 10 μm (Konda *et al.*, 2020). This NaCl aerosol-based testing is widely used for testing face respirators in compliance with the NIOSH 42 CFR Part 84 test protocol (Rengasamy *et al.*, 2018; eCFR, 2020). A recent study also used this aerosol generator to produce aerosolized saline for a quantified N95 fit test in order to evaluate a full-face snorkel mask with an airway circuit filter to protect healthcare providers against airborne pathogens (Kechli *et al.*, 2020). An aerosol monitor (DUSTTRAK™ II, Model 8532) measured the particle concentration before and after material filtration. An impactor (1 μm) was used along with the aerosol monitor to investigate the penetration of small droplets. Each sample was fitted to the sample holder and fastened by screws and rubber O-rings. The sample penetration was measured after 2 minutes of stabilization of the instrument. Measurements were recorded in the sampling holes perpendicular to the laminar flow of aerosol upstream and downstream of the samples. The concentration of NaCl droplet was recorded at a face velocity of 14 cm s^{-1}. The following equation calculated the filtration efficiency:

$$\eta_f = \left(1 - \frac{Particle\ Concentraion_{Downstream}}{Particle\ Concentraion_{Upstream}}\right) \times 100\% \quad (1)$$

where η_f is filtration efficiency. The background particle count was subtracted before calculation to cancel the factor of difference in particle concentration during the test.

2.1.3 Bactericidal test

Staphylococcus aureus (*S. aureus*) is a major cause of nosocomial and community-acquired infections. Infections caused by *S. aureus* remain a significant cause of mortality and morbidity in tropical countries (Onile *et al.*, 1985). A previous study showed that up to 80% of adults are found to harbor *S. aureus* in the nose (Wheat *et al.*, 1981). *S. aureus* is a gram-positive bacteria that is commonly used to demonstrate the efficiency of various disinfection methods. *S. aureus* (ATCC 25923) bacteria strain colony was inoculated using Nutrient Broth No. 2 (Thermo Scientific™ Oxoid™ Nutrient Broth No. 2 (dehydrated grade)) as an inoculating loop aseptically. The bacteria were then cultivated for 24 hours in an environmental shaker under a set of conditions (37°C, 200 rpm). This process ensured that the bacteria culture contained 10^{11} CFU L^{-1}. The bacteria culture was finally diluted to 10^9 CFU L^{-1} using a solution (0.9% saline and 0.1% Tween 80). The mask was divided into squares (1 × 1 inch) and put on a supporting glass plate of squares (1 × 1 inch) with the mask external layer material facing upward. A 50 μL of the diluted bacteria suspension was transferred onto each sample and the inoculum was dispersed evenly to allow the sample to be completely immersed in the solution. Three samples were selected randomly and applied for the aforementioned procedures. A timer was set to monitor the time exposure to the bacteria. After exposure, the sample was transferred to a sterile bottle containing 10 mL of extraction solution (0.9% saline and 0.1% Tween 80). The bottle was vortexed for 20 seconds, allowing sufficient time for the dislodgement of microbes into the solution. The suspension was serially diluted with different concentrations using sterilized saline solution (0.9%). 100 μL of the solution was inoculated onto TSA agar and cultured at 37°C for 24 hours. The colony forming units (CFUs) on agar plates were enumerated for analysis. The bactericidal efficiency was calculated by the following equation:

$$\eta_b = \left(1 - \frac{CFU\ retrieved\ after\ disinfection}{FU\ applied}\right) \times 100\% \quad (2)$$

where η_b is the bactericidal efficiency.

2.1.4 Hydrophobicity test

Five sets of 100 μL load of deionized (DI) water were added to a distance of 0.1 m above the sample at 5 different positions on the outer layer of the mask. The droplets were visually inspected for each sample. The mask was swirled gently and hydrophobicity was subsequently recorded for the water droplet shapes. Hydrophilicity was also recorded when water droplet shapes were in flattened (lowered contact angle) shapes but without penetration to all of the three layers. The damage to the water-repelling layer was checked and recorded when the water droplet was absorbed and penetrated to the bottom in the analysis.

2.1.5 Structural deformation analysis

Each sample's filtering layer (polypropylene) after treatments were sectioned to a size of 4 × 4 mm and fixed on a copper stage using carbon tapes. The samples were observed using a scanning electron microscope (SEM) (TM3000, Hitachi) and adjusted to suitable magnification (1000×). Structural changes (fiber diameter, melting, deformation, entanglement, or cracking of polypropylene fibers) were recorded in the analysis.

2.1.6 Data analysis

Comparison of the filtration efficiency as control (unused ASTM surgical mask) against filtration efficiency of the treatment group (re-used masks using different disinfection methods) was analyzed by paired t-test in SPSS (version 19.0) (IBM, 2023). p-value < 0.05 was set as significant.

2.2 Computer Simulation

2.2.1 Model construction

By simplifying a validated CFD model of a wardroom (Suen *et al.*, 2021), a 3D model size of 3 × 3 × 3 m was created to support airflow simulations in a conditioned indoor environment, as shown in Fig. S2. The Inlet and outlet of an air conditioner were modeled. Indoor heat sources, which are lamps and occupants, were included. Two occupants with noses were modeled to emit carbon dioxide (CO_2) and NaCl droplets. Since the CFD simulation aims to investigate the implied mask efficiency in an indoor environment based on the experimental results, the dispersion of NaCl droplets used in the lab test was included in the CFD. As presented in the Introduction, previous studies have indicated a correlation between CO_2 and the spatial dissipation of aerosols. The occupants were separated by 1.5 m. Masks were modeled as separated volumes to cover the bottom half of the faces of the occupants. The models were simplified to reduce computational costs.

2.2.2 Meshing

The mesh independence analysis of the CFD model was performed using unstructured mesh sizes of 0.54, 1.14, and 2.67 million. The growth rate of cells and the number of the boundary layer are set to be 1.2 and 10, respectively. Mesh independence was achieved when a mesh size of 1.14 million was used. Calculations made showed a mesh size of 1.14 million gave sufficient accuracy for the study with less than 4% difference in simulated results when the mesh size increases from 1.14 million and 2.67 million.

2.2.3 CFD simulation

Based on the Reynolds Averaged Navier Stokes (RANS) equations, Steady-state CFD simulations were conducted to simulate the dispersion of CO_2 and 2% NaCl droplets in an occupied and conditioned indoor environment. The software used in this study is ANSYS Fluent (ANSYS Inc., 2018). The advection scheme adopted is 2nd order upwind with the SST k-ω turbulent model to simulate airflow inside the room. The SST k-ω model was also used in previous studies of indoor

CFD simulations to simulate reasonably accurate indoor airflow (Hussain *et al.*, 2012; Gilani *et al.*, 2016; Wu *et al.*, 2020). It uses a blending function to combine the strengths of standard k-ε and standard k-ω models. As a result, the standard k-ε model was applied in a fully turbulent freestream, whereas the standard k-ω model was used in the near-wall region. The blending function of the SST k-ω model is useful in this study for simulating both airflows near the walls and inside different regions on the floor. Table S2 presents the boundary conditions in the CFD simulations. The settings of the air conditioner are based on the field measurement conducted in a palliative care facility (Suen *et al.*, 2021). This study assumes that the air conditioner does not recirculate used air as recommended by the current guidelines (Guo *et al.*, 2021). The masks were modeled as air volumes with resistance. Based on experimental results from Table 1, the resistance of masks was calculated as friction factors(f_p) using the Ergun equation:

$$f_p = \frac{\Delta p}{L}\frac{D_p}{\rho \upsilon_s^2}\left(\frac{\epsilon^3}{1-\epsilon}\right) \tag{3}$$

where Δp is the pressure drop across the mask volume, L is the distance between the nose and the mask, D_p is the equivalent spherical diameter of the mask volume, ρ is the density of air, υ_s is the superficial velocity (i.e., the velocity that air would have through without mask) and ϵ is the porosity of the mask.

2.2.4 Scenario study

10 cases were studied to quantify the effectiveness of masks. For each of the 3 masks, there are 3 different cases: (1) both occupants wear masks; (2) one of the occupants wears a mask; and (3) another occupant wears a mask. This is to observe the variations of mask effectiveness when different masks are considered. Apart from the nine cases, a case in which none of the occupants wear masks is included, in order to determine the effect of mechanical ventilation on mask effectiveness. The simulated results of 2% NaCl droplets and CO_2 concentration distribution from different cases will be compared.

3 RESULTS AND DISCUSSION

3.1 Effectiveness of Masks under Experimental Treatments

Three unused masks were tested for filtration efficiency using NaCl droplets. The results from Table 1 show that samples 1 and 2 filtration efficiencies are 98.7 and 97.0%, respectively. Sample 3 shows the highest filtration efficiency (99.9%) in this analysis. The differences could be potentially due to the mask density. The analysis shows higher density with higher filtration efficiency.

3.2 Impact of Mechanical Ventilation on the Effectiveness of Masks

Fig. 2 presents the distribution of 2% NaCl droplets on the nose level. Based on the experiment results, the filtration efficiency of the sample masks is around 97–99%. In all cases where occupants are wearing masks, the concentration of NaCl droplets is less than 0.2 mg m^{-3} on average in the room except for the air volume inside the masks. As 5.24 × 10^{-3} g m^{-3} of NaCl droplets have been dissipated from the occupants, less than 4% of the droplets remain in the room on average. Therefore, the simulated results are considered to agree with the experimental results.

Table 1. Physical characteristics of masks (n = 3 for each type of mask).

Sample number	Sample description	Filtration efficiency (η_f)	Pressure drop (ΔP kPa)	Velocity (m s^{-1})	Dimensions		Weight	Density
					Area (cm^2)	Thickness		
1	ASTM Level 1 surgical mask	98.67%	0.200	0.360	22.373	0.410	0.202	0.022
2	Surgical mask without certification	97.03%	0.200	0.390	22.178	0.370	0.201	0.024
3	KF94 mask	99.90%	0.210	0.270	22.141	0.570	0.360	0.028

https://doi.org/10.4209/aaqr.230123

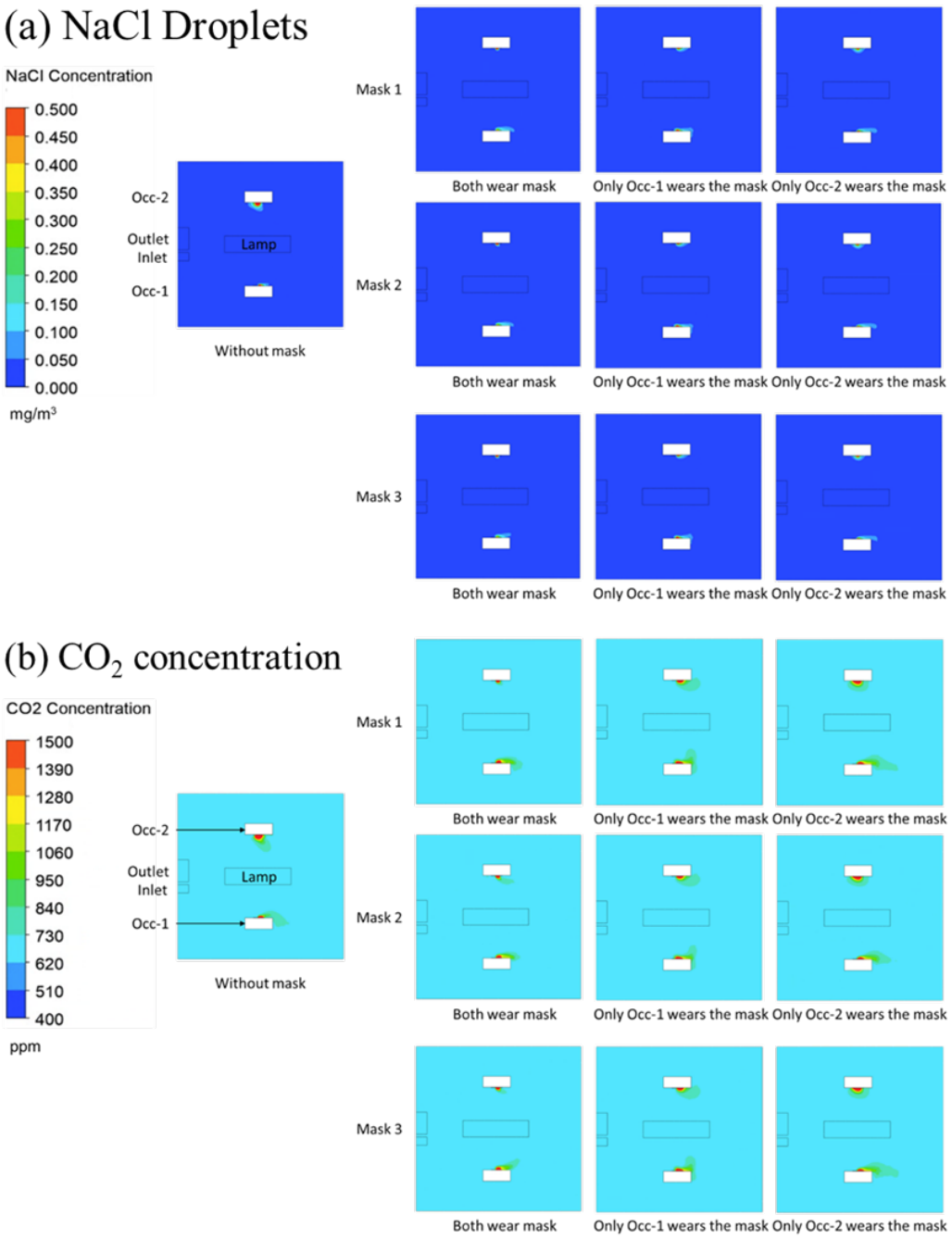

Fig. 2. Simulated result of concentration distribution of (a) NaCl droplets and (b) CO_2 on nose level.

Figs. 3(a) and 3(b) present the average concentration of NaCl droplets and CO_2 in the sample room in different cases. Overall CO_2 concentration in the room is well above 400 ppm and below 800 ppm. The air in the room is well-mixed and the ventilation is satisfactory. The occupants' cognitive functions are unaffected as the CO_2 concentration does not exceed 1000 ppm. Airflow patterns affect the efficiency of masks. Disabling air recirculation and wearing masks are effective to reduce the overall concentration of NaCl droplets. As the room supplies only conditioned fresh air, this disables air recirculation and prevents NaCl droplets accumulation in the room.

While masks are generally effective to reduce the accumulation and dispersion of CO_2 and NaCl in front of masks in most the cases, the simulated results indicate that the accumulation of NaCl is less significant than CO_2, by comparing the simulated results presented in Figs. 2(a) and 2(b). In the case of without any mask-wearing, NaCl droplets are accumulated in front of Occupant-2 (Occ-2).

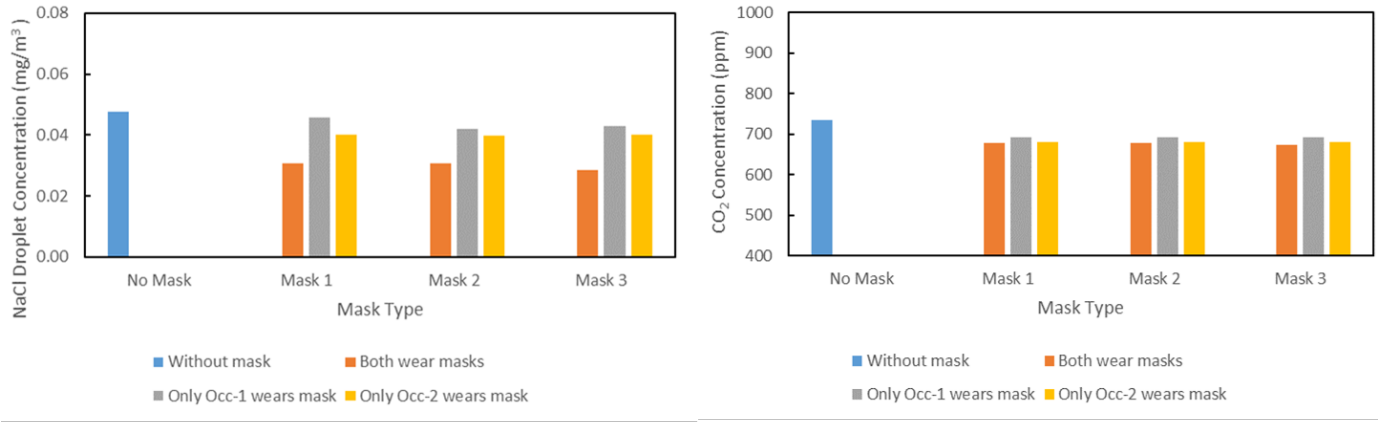

(a) NaCl Droplets (b) CO_2 concentration

Fig. 3. Average concentration of (a) NaCl droplets and (b) CO_2 in the sample room.

The red spot disappears in the cases with mask-wearing. Dispersion of CO_2 and NaCl droplets is more prominent around Occupant-1 (Occ-1), where the inlet of the air conditioner induces airflow. As supply airflow moves faster than return airflow, the dispersion is more obvious around Occ-1 than Occ-2. The effectiveness of masks is reduced substantially.

3.3 Effectiveness of Masks under Reusability Treatments

3.3.1 Filtration efficiency

All samples were tested for filtration efficiency. Control samples show average filtration efficiency of 98.67 % ± 0.21 % at 0.13 m s^{-1}. The average filtration efficiencies for different sets (household detergent, after water and ethanol treatment) of samples are lower than the control. Samples after boiling, steaming, autoclave and UVC irradiation are slightly different from the control value. After one treatment cycle, all treatment methods except UVC irradiation demonstrate a decrease in filtration efficiency. In Table 2, treatment with household detergent and ethanol show a significant decrease in filtration efficiency. After three treatment cycles, the UVC irradiation and dry heated samples are to retain high filtration efficiencies (> 97%). The paired t-test results show statistically significant differences ($p < 0.005$) for all disinfection treatments except for the UVC irradiation (after 3 treatment cycles). This implies the filtration efficiency has significantly been reduced compared to the control setting. The non-fluid treatments show better performance

Table 2. Physical performance of masks after control and treatments.

Method	Untreated (Control)		One treatment cycle				Three treatment cycles			
	η_f[1]	σ[2]	η_f	σ	p[3]	Hydrophobicity	η_f	σ	p	Hydrophobicity
Control treatment	98.67%	0.21%				Bead-like droplets				Bead-like droplets
Boiling			94.99%	0.53%	$p < 0.005$	Flatten droplets	94.83%	3.70%	$p < 0.005$	Flatten droplets
Steaming			98.00%	0.24%	$p < 0.005$	Flatten droplets	96.15%	1.30%	$p < 0.005$	Flatten droplets
Autoclave			95.73%	0.71%	$p < 0.005$	Flatten droplets	92.24%	0.60%	$p < 0.005$	Flatten droplets
Household detergent			77.89%	2.86%	$p < 0.005$	Penetrated	74.41%	1.50%	$p < 0.005$	Penetrated
75% Ethanol			84.64%	1.67%	$p < 0.005$	Flatten droplets	82.93%	1.00%	$p < 0.005$	Flatten droplets
95% Ethanol			82.62%	2.61%	$p < 0.005$	Flatten droplets	78.11%	5.70%	$p < 0.005$	Flatten droplets
Dry heating			97.86%	0.14%	$p < 0.005$	Bead-like droplets	97.72%	0.90%	$p < 0.005$	Bead-like droplets
UVC[4] irradiation			97.56%	0.31%	$p < 0.005$	Bead-like droplets	98.55%	0.40%	$p > 0.005$	Bead-like droplets

[1] η_f stands for filtration efficiency.
[2] σ stands for standard deviation.
[3] p stands for statistical measurement used to validate a hypothesis against observed data.
[4] UVC stands for ultraviolet light.

than fluid-based treatments in filtration efficiency tests. The possible explanation can be because of the neutralization of electric charges of polypropylene filtration layer after using organic solvents (Choi *et al.*, 2015).

3.3.2 Disinfection efficiency

According to Table 3, all of the methods (boiling, steaming, ethanol treatment and dry heating) are effective in reducing the *S. aureus* (99.99%). Irradiation with UVC can also provide the same disinfection performance. Except for household detergent treatment, all disinfection methods are effective in eliminating *S. aureus* on the mask materials. The detergent used in this study shows no bactericidal effect on *S. aureus*. The reduction efficiency can be potentially due to the partial suspension of bacteria in solution. Disinfection methods (boiling, steaming, ethanol treatment, dry heating and UVC irradiation) are effective to control microbial growth and further to reduce the risk of recontamination when reusing the mask after treatments.

Moist (boiling, steaming and autoclave) and dry heating treatments (dry heating and UVC irradiation) are classified in the analysis. Dry heating treatment is slower than moist heating treatment. Nevertheless, dry heating (100°C for 15 minutes) treatment is able to achieve a 99.99% reduction for *S. aureus*. Ethanol (60–95%) treatment can cause protein denaturation and further microorganisms dehydration (Block, 2001). The results show 99.99% reduction for *S. aureus* in 5 minutes. UVC irradiation (254 nm) is a method that uses electromagnetic radiation to damage ribonucleic acid (RNA), deoxyribonucleic acid (DNA) and protein. The result shows an exposure to UVC irradiation (450 μW cm^{-2} for 10 minutes) can effectively eliminate all *S. aureus* on the mask materials.

3.3.3 Hydrophobicity test

In Table 2, droplets with bead shapes were used to test in non-fluid disinfection methods (dry heating and UVC irradiation). Dry heating and UVC irradiation show no observable effect on the hydrophobicity of mask surface. All other disinfection treatments in this study cause damage to the fluid-repelling layers as the water droplets on the mask surface cannot be retained to the bead shape. For household detergent treatment, water is not able to completely remove detergent from the mask materials. The masks after detergent treatment demonstrate severe water penetration and this observation can possibly be related to lower surface tension caused by surfactants (Ciborowski and Silberring, 2016). The samples demonstrate flattened droplets in the other treatments (boiling, steaming, autoclave and ethanol treatment). The results can be possibly related to the loss of structure conformation after treatments. The results of hydrophobicity reflect the existence of the hydrophobic layer and the strength of filtering out virus-containing droplets.

Table 3. Statistical summary of fiber diameter and reduction efficiency under different disinfection methods.

Method	Average Fibre Diameter	σ[1]	*p*[2]	Reduction Efficiency	σ[1]
Control treatment	0.0277	0.0046916	N.A.	N.A.	N.A.[3]
Boiling	0.0315	0.0132099	$p > 0.05$	99.99%	± 0.00%
Steaming	0.0354	0.0157917	$p > 0.05$	99.99%	± 0.00%
Autoclave	0.0356	0.0123576	$p > 0.05$	99.99%	± 0.00%
Household Detergent	0.0290	0.0125875	$p > 0.05$	50.86%	± 9.20%
75% Ethanol	0.0491	0.0209839	$p < 0.05$	99.99%	± 0.00%
95% Ethanol	0.0434	0.0134014	$p < 0.05$	99.99%	± 0.00%
Dry heating	0.0270	0.0042688	$p > 0.05$	99.99%	± 0.00%
UVC[4] irradiation	0.0259	0.0051521	$p > 0.05$	99.99%	± 0.00%

[1] σ stands for standard deviation.
[2] *p* stands for statistical measurement used to validate a hypothesis against observed data.
[3] N.A. indicates not available.
[4] UVC stands for ultraviolet light.

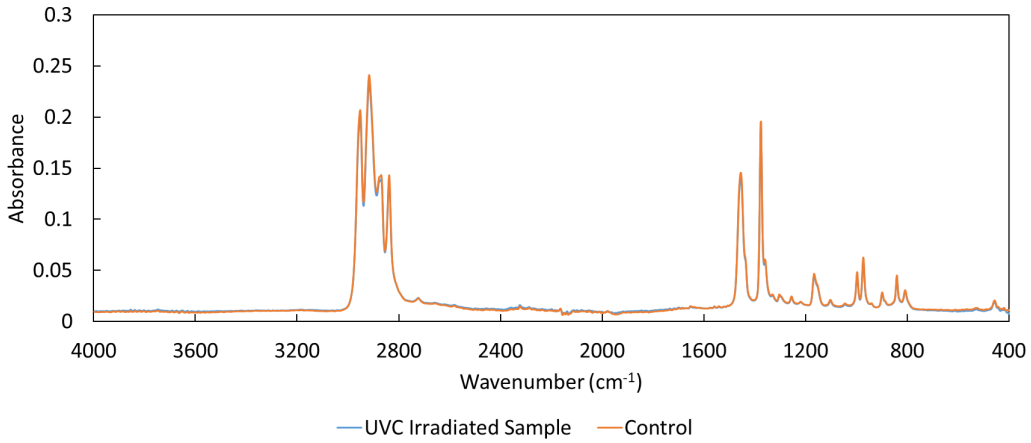

Fig. 4. Fourier-transform infrared spectroscopy (FTIR) spectrum of surgical mask (filtration layer). Orange curve denotes control sample and blue curve denotes UVC treated sample after UVC irradiation (450 μW cm^{-2} for 90 minutes).

3.3.4 Structural changes

All ear loops on the masks remain unchanged throughout the experiment, except for the samples after boiling, steaming and autoclave. The samples after boiling and steaming show softened texture on the mask surface. UVC irradiation shows no damage to the filtration layer even after 90 minutes of exposure to the radiation. Although UVC irradiation is proven to facilitate the degradation of polypropylene, nevertheless, the short time exposure used for disinfection cannot cause significant structural damage to the filtration layer (Shimizu *et al.*, 2016). This observation was further confirmed by Fourier-transform infrared spectroscopy (FTIR) in Fig. 4. The result shows no significant differences between control and samples after treatments.

All of the abovementioned disinfection methods show no observable damage to the samples, except for the samples after steaming and boiling treatment. The samples are noticeably tarnished and softened after the analysis. The SEM images presented in Fig. 5 reveal no structural change to the filtering layer in all disinfection methods. There are no shrink, melt, deformation, entanglement and cracks of fibers in the analysis. Peelings are observed from the outer surface of fibers for the samples after UVC irradiation. UVC radiation is in the highest energy section of the UV radiation spectrum that can cause deterioration of fibers in the samples.

In Table 3, the paired t-test result shows insignificant differences between the control and treatments (except for ethanol (75 and 95%) treatment). This implies other than alcohol-based treatment, fiber diameter shows no significant increase after treatment. However, the standard deviation (except in dry heating and UVC irradiation) demonstrates an increase compared to the control. This observation can possibly be due to fluid disinfection method poses irregular structural conformation for the mask.

3.3.5 Implication of experimental results

The COVID-19 pandemic causes large demand of surgical masks worldwide. Mask disinfection is an alternative approach to ensure enough supply. The experiment section is to identify disinfection methods that can cause least damage to the mask using different analysis (the overall mask integrity, hydrophobicity and filtration efficiency). The methods are further required to eliminate harmful microorganisms with high reproducibility. The safety of mask reuse is paramount after treatment. Other gas disinfection treatments (e.g., chlorine and ozone gas) are not recommended due to their potential hazards. Ozone gas is toxic to mankind. This substance is not recommended to use in an area without sufficient ventilation (WHO, 2021). Chlorine gas and other chlorinated compounds can react with polypropylene to generate harmful by-products (HMC Polymers, 2012). This may potentially cause damage to the surface characteristics of the mask. There is also a limitation to use aqueous bleach solution (1:99) for disinfection as the solution alone cannot be used to fully submerge the mask to provide thorough disinfection.

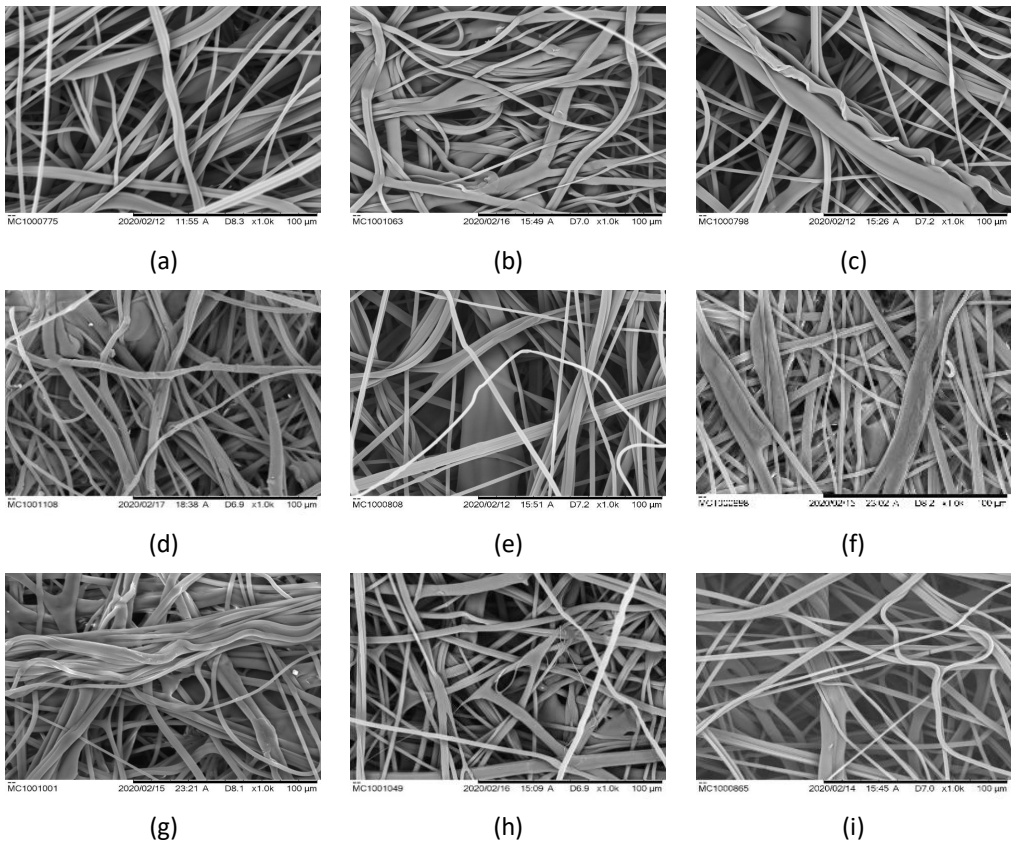

Fig. 5. Appearance of mask filtration layers after disinfection treatments under scanning electron microscope (1000×): (a) control sample; (b) boiled sample; (c): steamed sample; (d) autoclaved sample; (e) detergent treated sample; (f) ethanol (75%) treated sample; (g) ethanol (95%) treated sample; (h) dry heated sample; (i) UVC irradiated sample.

Two non-fluid treatments (UVC irradiation and dry heating) were identified to maintain the highest performance compared to the others in terms of filtration efficiency, structural consistency and sufficient hydrophobicity (three treatment cycles). Dry heating is a disinfection method suitable for household use.

3.4 Mask Effectiveness Results of new Masks and Reused Masks in Indoor Environment

To quantify mask effectiveness for the new masks in a conditioned and occupied indoor environment, reduction in overall NaCl and CO_2 levels in the sample room was calculated based on the comparison of simulated results of the cases with both occupants wearing masks and the case with them without masks. Fig. 6 presents the results and compares them with the corresponding filtration efficiency measured in the experiments. The reduction in overall NaCl and CO_2 levels is directly proportional to the filtration efficiency. To quantify mask effectiveness for the reused masks in an indoor environment, the reduction in overall NaCl and CO_2 levels is calculated based on the results of new masks and the corresponding measured filtration efficiency. Therefore, the projected effectiveness of reused masks is also directly proportional to the filtration efficiency, which is the same as the new masks. The masks, which are disinfected with household detergent, 75% ethanol and 95% ethanol, can only block less than 30% of NaCl droplets on average. The reduction in the overall NaCl level of reused masks is generally less significant than the new masks because of the lower filtration efficiency. As for the reduction in CO_2 level, all masks can only reduce by less than 10%. This indicates that the breathing of occupants is unaffected in general. However, airborne transmission is possible if the aerosol particles are much smaller than the NaCl droplets.

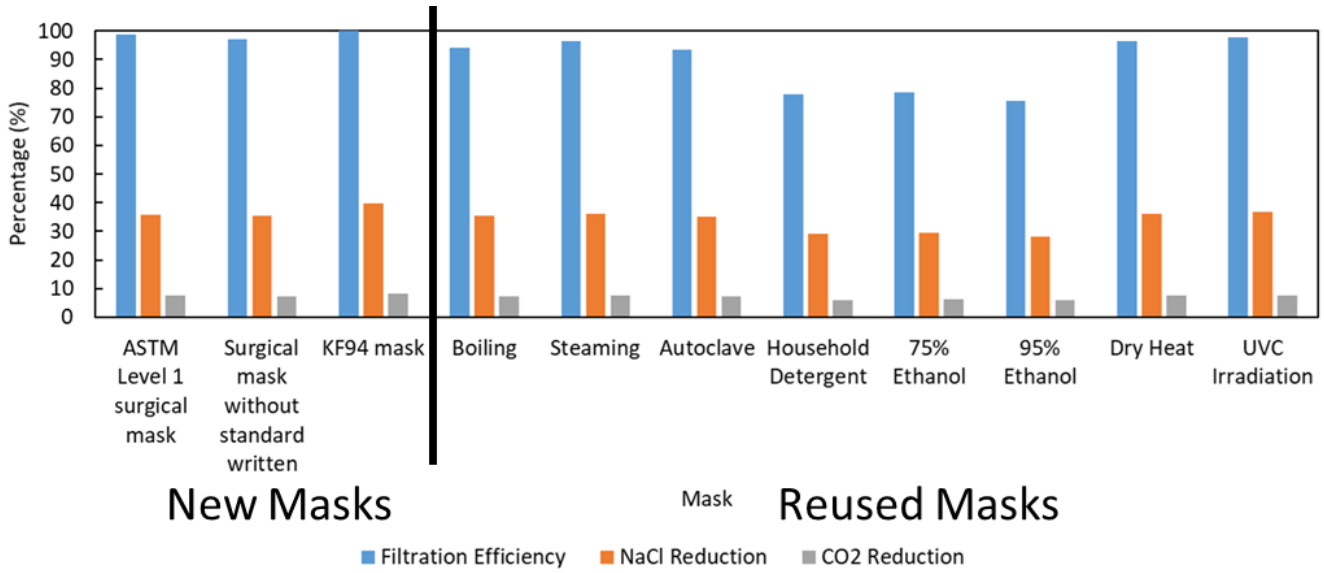

Fig. 6. Mask effectiveness of sample masks based on experimental and simulated results.

3.5 Impact of Mode of Transmission on the Effectiveness of Mask and Social Distancing

The main transfer pathway of SARS-CoV-2 is via exposure to the respiratory fluid that carries the infectious virus. The three major exposure routes are inhalation of the very fine respiratory droplets and aerosol particles, deposition of respiratory droplets and touching with hands (Yu *et al.*, 2004; Li *et al.*, 2005; Otter *et al.*, 2016). In the CFD simulation, CO_2 was considered a surrogate indicator for aerosol particles. Based on Fig. 3, the CO_2 concentration in the room is slightly lower under the three scenarios (either one occupant or both of them wear masks). This observation suggests that masks can slightly reduce the accumulation of the exhaled respiratory fluid in the air space under adequate ventilation. However, the CO_2 concentrations for all cases are all above 650 ppm after the model reaches equilibrium under the initial condition (400 ppm). This shows the very fine respiratory droplets penetrate the mask after a period of time. The CO_2 concentration increase shows that aerosol particles are accumulated under adequate ventilation and further pose the risk of infection. In Fig. 2(b), the CO_2 concentration decreases rapidly after emissions which demonstrates the virus is uniformly mixed and dispersed. By comparing wearing masks and not wearing masks, a higher concentration of CO_2 is observed near the mouth regions of occupants when masks are worn. This suggests that the mask slows the dispersion of exhaled respiratory fluid and changes the direction of dispersion. Under the without mask cases, the area of high CO_2 concentration is larger, which implies the aerosol particles require a longer distance to thoroughly mix with the surroundings. As a result, although adequate ventilation is provided to an indoor environment, there is a higher possibility of infection in the case without masks and the risk of infection is still present when masks are worn.

Aside from CO_2, the NaCl droplets (2%) are further used to simulate the deposition of respiratory droplets. Based on Fig. 2(a), the average NaCl droplet concentration significantly decreases when both occupants wear masks, and slightly decreases when only one occupant wears masks. This supports that the velocity of respiratory droplets is reduced by masks and mainly contained in the mask. In Fig. 3(a), the NaCl droplet concentrations in all conditions are higher than 3% after the model reaches equilibrium. This supports that part of the respiratory droplet has infiltrated the mask after a period of time. In Fig. 6, the NaCl droplet reduction is 20% higher than CO_2 reduction, which demonstrates that the mask has a higher ability on blocking the NaCl droplet and its penetration. In conclusion, for an indoor environment with adequate ventilation, wearing masks effectively reduces the risk of infection via respiratory droplets compared with aerosol particles. Nevertheless, the risk of infection cannot be neglected due to the accumulation of respiratory droplets in air space.

4 CONCLUSION

An experimental coupled with a computational approach is proposed to quantify the effectiveness of masks in an indoor environment with occupants. Several disinfection methods were investigated based on mask integrity, hydrophobicity and filtration efficiency in order to evaluate the overall reusability of masks. Two non-fluid contacting disinfection methods, namely UVC irradiation and dry heating, were identified as the most effective in terms of filtration efficiency, structural consistency and sufficient hydrophobicity after three rounds of disinfection treatments, compared to the other test methods.

The simulated results are considered to agree with the experimental results in general. For each case in the scenario study, it takes about 1 hour for a 12-core Intel Xeon 6126, which is less powerful than an Intel i5-12400. Therefore, the proposed methodology can be used with a typical desktop computer assembled this year to quantify the effectiveness of different types of masks. While masks are generally effective to reduce the accumulation and dispersion of CO_2 and NaCl in front of masks in most cases, the simulated results indicate that the accumulation of NaCl is less significant than CO_2.

The results indicate the factors causing the infection are poor ventilation, poor mask fitting and infectiveness of the virus. Several limitations of this study are observed due to: (1) human movement was ignored; (2) temporal variations of CO_2 and NaCl droplets were not considered; and (3) comfort levels of reused masks are not considered as many people have already worn reused masks before our experiment based on our observation. Further study will be required to quantify the viral loading in the air to cause infection, consider different types of masks and comfort levels of reused masks, as well as investigate different viruses, bacteria, and pathogens.

ACKNOWLEDGMENTS

This study was supported by the Research Grants Council of the Hong Kong Special Administrative Region China, General Research Fund (Project No. 14203719).

SUPPLEMENTARY MATERIAL

Supplementary material for this article can be found in the online version at https://doi.org/10.4209/aaqr.230123

REFERENCES

ANSYS Inc. (2018). Ansys Fluent, https://www.ansys.com/products/fluids/ansys-fluent, access Last Access: 15 April 2023.

ASTM International (2017). F2299-03 Standard Test Method for Determining the Initial Efficiency of Materials Used in Medical Face Masks to Penetration by Particulates Using Latex Spheres, ASTM International, West Conshohocken, Pennsylvania.

Block, S.S. (2001). Disinfection, Sterilization, and Preservation, 5th ed. Lippincott Williams and Wilkins, Philadelphia.

Chen, H., Janbakhsh, S., Larsson, U., Moshfegh, B. (2015). Numerical investigation of ventilation performance of different air supply devices in an office environment. Build. Environ. 90, 37–50. https://doi.org/10.1016/j.buildenv.2015.03.021

Chen, Q.Y. (2009). Ventilation performance prediction for buildings: a method overview and recent applications. Build. Environ. 44, 848–858. https://doi.org/10.1016/j.buildenv.2008.05.025

China Food and Drug Administration (CFDA) (2011). Surgical Mask Yy0469-2011. Pharmaceutical Industry Standard, China.

Choi, H.J., Park, E.S., Kim, J.U., Kim, S.H., Lee, M.H. (2015). Experimental study on charge decay of electret filter due to organic solvent exposure. Aerosol Sci. Technol. 49, 977–983. https://doi.org/10.1080/02786826.2015.1086724

Ciborowski, P., Silberring, J. (2016). Proteomic Profiling and Analytical Chemistry: The Crossroads. Elsevier.

Electronic Code of Federal Regulations (eCFR) (2020). Title 42: Public Health, Part 84—Approval of Respiratory Protective Devices. Code of Federal Regulations.

Feng, Y., Marchal, T., Sperry, T., Yi, H. (2020). Influence of wind and relative humidity on the social distancing effectiveness to prevent COVID-19 airborne transmission: A numerical study. J. Aerosol Sci. 147, 105585. https://doi.org/10.1016/j.jaerosci.2020.105585

Gilani, S., Montazeri, H., Blocken, B. (2016). CFD simulation of stratified indoor environment in displacement ventilation: Validation and sensitivity analysis. Build. Environ. 95, 299–313. https://doi.org/10.1016/j.buildenv.2015.09.010

Guo, M., Xu, P., Xiao, T., He, R., Dai, M., Miller, S.L. (2021). Review and comparison of HVAC operation guidelines in different countries during the COVID-19 pandemic. Build. Environ. 187, 107368. https://doi.org/10.1016/j.buildenv.2020.107368

HMC Polymers (2012). Polypropylene Chemical Resistance Guide, HMC Polymers, Thailand, pp. 1–9.

Hussain, S., Oosthuizen, P.H., Kalendar, A. (2012). Evaluation of various turbulence models for the prediction of the airflow and temperature distributions in atria. Energy Build. 48, 18–28. https://doi.org/10.1016/j.enbuild.2012.01.004

IBM (2023). Spss Software, https://www.ibm.com/analytics/spss-statistics-software (accessed 15 April 2023).

Ishack, S., Lipner, S.R. (2020). Applications of 3D printing technology to address COVID-19–related supply shortages. Am. J. Med. 133, 771–773. https://doi.org/10.1016/j.amjmed.2020.04.002

Jung, H., Kim, J.K., Lee, S., Lee, J., Kim, J., Tsai, P., Yoon, C. (2014). Comparison of filtration efficiency and pressure drop in anti-yellow sand masks, quarantine masks, medical masks, general masks, and handkerchiefs. Aerosol Air Qual. Res. 14, 991–1002. https://doi.org/10.4209/aaqr.2013.06.0201

Kechli, M.K., Lerman, J., Ross, M.M. (2020). Modifying a full-face snorkel mask to meet N95 respirator standards for use with coronavirus disease 2019 patients. A A Pract. 14, e01237, https://doi.org/10.1213/xaa.0000000000001237

Khosronejad, A., Santoni, C., Flora, K., Zhang, Z., Kang, S., Payabvash, S., Sotiropoulos, F. (2020). Fluid dynamics simulations show that facial masks can suppress the spread of COVID-19 in indoor environments. Aip Adv. 10, 125109. https://doi.org/10.1063/5.0035414

Konda, A., Prakash, A., Moss, G.A., Schmoldt, M., Grant, G.D., Guha, S. (2020). Aerosol filtration efficiency of common fabrics used in respiratory cloth masks. Acs Nano 14, 6339–6347. https://doi.org/10.1021/acsnano.0c03252

Kwok, H.H.L., Cheng, J.C.P., Li, A.T.Y., Tong, J.C.K., Lau, A.K.H. (2022). Impact of shaft design to thermal comfort and indoor air quality of floors using bim technology. J. Build. Eng. 51, 104326. https://doi.org/10.1016/j.jobe.2022.104326

Li, Y., Huang, X., Yu, I., Wong, T., Qian, H. (2005). Role of air distribution in sars transmission during the largest nosocomial outbreak in Hong Kong. Indoor Air 15, 83–95. https://doi.org/10.1111/j.1600-0668.2004.00317.x

National Institute for Occupational Safety & Health (NIOSH) (2007). Determination of Particulate Filter Efficiency Level for N95 Series Filters against Solid Particulates for Non-Powered, Air-Purifying Respirators Standard Testing Procedure (STP). National Institute for Occupational Safety & Health, Pittsburgh, Pennsylvania. https://www.cdc.gov/niosh/npptl/stps/pdfs/TEB-APR-STP-0059-508.pdf

Nielsen, P.V. (2015). Fifty years of CFD for room air distribution. Build. Environ. 91, 78–90. https://doi.org/10.1016/j.buildenv.2015.02.035

Onile, B., Odugbemi, T., Nwofor, C. (1985). Antibiotic susceptibility of Bacterial agents of Septicemia in Ilorin. Nig. Med. Pract. 9, 16–18.

Otter, J.A., Donskey, C., Yezli, S., Douthwaite, S., Goldenberg, S., Weber, D. (2016). Transmission of SARS and MERS coronaviruses and influenza virus in healthcare settings: the possible role of dry surface contamination. J. Hosp. Infect. 92, 235–250. https://doi.org/10.1016/j.jhin.2015.08.027

Rengasamy, S., Shaffer, R., Williams, B., Smit, S. (2017). A comparison of facemask and respirator

filtration test methods. J. Occup. Environ. Hyg. 14, 92–107. https://doi.org/10.1080/15459624.2016.1225157

Rengasamy, S., Zhuang, Z., Niezgoda, G., Walbert, G., Lawrence, R., Boutin, B., Hudnall, J., Monaghan, W.P., Bergman, M., Miller, C., Harris, J., Coffey, C. (2018). A comparison of total inward leakage measured using sodium chloride (NaCl) and corn oil aerosol methods for air-purifying respirators. J. Occup. Environ. Hyg. 15, 616–627. https://doi.org/10.1080/15459624.2018.1479064

Rivas, E., Santiago, J.L., Martín, F., Martilli, A. (2022). Impact of natural ventilation on exposure to SARS-CoV 2 in indoor/semi-indoor terraces using CO_2 concentrations as a proxy. J. Build. Eng. 46, 103725. https://doi.org/10.1016/j.jobe.2021.103725

Schade, W., Reimer, V., Seipenbusch, M., Willer, U. (2021). Experimental investigation of aerosol and CO_2 dispersion for evaluation of COVID-19 infection risk in a concert hall. Int. J. Environ. Res. Public Health 18, 3037. https://doi.org/10.3390/ijerph18063037

Shimizu, K., Tokuta, Y., Oishi, A., Kuriyama, T., Kunioka, M. (2016). Weatherability of polypropylene by accelerated weathering tests and outdoor exposure tests in Japan. J. Polym. 2016, 6539567. https://doi.org/10.1155/2016/6539567

Suen, C.Y., Lai, Y.T., Lui, K.H., Li, Y., Kwok, H.H.L., Chang, Q., Lee, J.H., Han, W., Yang, X., Yang, Z., Mo, Z., Wong, P.K.S., Leung, A.C.T., Kwan, J.K.C., Yeung, K.L. (2021). Virucidal, bactericidal, and sporicidal multilevel antimicrobial HEPA-ClO_2 filter for air disinfection in a palliative care facility. Chem. Eng. J. 433, 134115. https://doi.org/10.1016/j.cej.2021.134115

Wheat, L.J., Kohler, R.B., White, A. (1981). Treatment of Nasal Carriers of Coagulase-Positive Staphylococci, In Skin Microbiology, Springer, pp. 50–58.

World Health Organization (WHO) (2020). Advice on the use of masks in the context of COVID-19. Interim Guidance, 6 April 2020. World Health Organization. https://apps.who.int/iris/handle/10665/331693

World Health Organization (WHO) (2021). Review of evidence on health aspects of air pollution: REVIHAAP project: technical report. World Health Organization. Regional Office for Europe. https://apps.who.int/iris/handle/10665/341712

World Health Organization (WHO) (2023). Coronavirus Disease (Covid-19): Masks. https://www.who.int/emergencies/diseases/novel-coronavirus-2019/question-and-answers-hub/q-a-detail/coronavirus-disease-covid-19-masks (accessed 15 April 2023).

Wu, J., Li, X., Lin, Y., Yan, Y., Tu, J. (2020). A PMV-based HVAC control strategy for office rooms subjected to solar radiation. Build. Environ. 177, 106863. https://doi.org/10.1016/j.buildenv.2020.106863

Xie, X., Li, Y., Chwang, A., Ho, P., Seto, W. (2007). How far droplets can move in indoor environments--revisiting the Wells evaporation-falling curve. Indoor Air 17, 211–225. https://doi.org/10.1111/j.1600-0668.2007.00469.x

Yang, Y., Wang, Z., Li, X., Wang, H., Ren, Y., Zhao, D., Xu, Z. (2021). Test and simulation for the airtightness of backdraft dampers in residential cooking exhaust shaft systems. J. Build. Eng. 44, 103007. https://doi.org/10.1016/j.jobe.2021.103007

Yu, I.T., Li, Y., Wong, T.W., Tam, W., Chan, A.T., Lee, J.H., Leung, D.Y., Ho, T. (2004). Evidence of airborne transmission of the severe acute respiratory syndrome virus. N. Engl. J. Med. 350, 1731–1739. https://doi.org/10.1056/NEJMoa032867

Zhang, M., Shrestha, P., Liu, X., Turnaoglu, T., DeGraw, J., Schafer, D., Love, N. (2022a). Computational fluid dynamics simulation of SARS-CoV-2 aerosol dispersion inside a grocery store. Build. Environ. 209, 108652. https://doi.org/10.1016/j.buildenv.2021.108652

Zhang, T., He, M., Li, B., Zhang, C., Hu, J. (2022b). Acoustic characteristics of cantonese speech through protective facial coverings. J. Voice https://doi.org/10.1016/j.jvoice.2022.08.029